Automatic Drift Correction through Nonlinear Sensing

1st Dhrubajit Chowdhury
Sensors and Controls Group
Oak Ridge National Laboratory
Oak Ridge, USA
0000-0002-9113-0323

1st Alexander Melin
Sensors and Controls Group
Oak Ridge National Laboratory
Oak Ridge, USA
0000-0002-7120-8154

2nd Kris Villez
Sensors and Controls Group
Oak Ridge National Laboratory
Oak Ridge, USA
0000-0002-8330-010X

***Abstract*—For successful design and operation of advanced monitoring and control systems, engineers rely on high quality sensor signals that are simultaneously accurate, representative, voluminous, and timely. Unfortunately, sensor faults are common and lead to short-lived symptoms, such as outliers and spikes as well as long-lived symptoms, such as sensor drift. Sensor drift belongs to the category of incipient faults. These are particularly challenging to detect, diagnose, and correct as the time scales of these faults are typically longer than the time scales of the system dynamics that are of interest. Moreover, if sensor drift occurs as a result of exposure to measured medium, then it is likely that multiple sensors will exhibit similar drift rates, thus challenging fault management strategies based on redundancy. In this contribution, we present a first method that can handle this unique challenge.**

***Index Terms*—Auto-calibration, Fault correction, Incipient fault, Observer, Sensor drift, Unscented Kalman filter**

I. INTRODUCTION

In many areas of engineering, special attention is given to ubiquitous sensing as a way to gather information at ever-increasing spatial and temporal resolutions [1]. This is at least partly motivated by successes in machine learning, particularly in image classification and machine translation, which is a result of novel algorithms, specialized hardware, and massive data sets (see e.g., [2], [3]).

Unfortunately, successful deployment of predictive modelling of any kind requires access to high quality data sets that are representative for the scenarios where the model-based prediction will be used. Collecting such data sets can be a serious challenge [4]. For example, data-driven models for anomaly detection can be hard to establish if the anomalies of interest occur rarely or are otherwise mitigated through human or automated interventions.

Another challenge consists of incipient sensor faults, like drift. The most successful methods available today are based on redundancy, which is either established based on first principles (e.g., mass balances) or based on correlations (e.g., principal component analysis). This however assumes that drift faults do not start simultaneously in every sensor or that the drift rates in the deployed sensors are sufficiently different from each other. For some sensors, like those based on ion-selective electrodes (ISE), neither requirement is met. Indeed, [5] show empirically that redundant sensors exposed to the same medium likely exhibit drift at the same time with the same rate, especially if they are constructed the same. This severely limits the utility of redundancy-based algorithms for fault detection. Following the above negative conclusion, [5] suggest to develop and study methods that can detect incipient faults, like sensor drift, but do not rely on the assumption that incipient faults appear independently and with dissimilar magnitudes.

This contribution is a first attempt to address the need identified above. To this end, we test a rather simple yet novel approach, consisting of deliberate placement of differential pressure sensors in a water reservoir at different heights. We show that a nonlinear observer can be used to estimate the sensor offset in every sensor. This is feasible thanks to the discontinuous response curve of the sensors used to measure the water level in the reservoir. The discontinuity appears at a different water level for each sensor, which makes its location identifiable whenever the water level crosses one of the sensor's locations.

This material is in part based upon work supported by the National Alliance for Water Innovation (NAWI), funded by the U.S. Department of Energy, Energy Efficiency and Renewable Energy Office, Advanced Manufacturing Office under Funding Opportunity Announcement DE-FOA-0001905.

II. Materials and Methods

In the following sections, the general method is explained first (Sections A). After (Section B), we explain the simulation study to illustrate the benefits of the proposed method.

A. Method

1) System model: Our method is based on the unscented Kalman filter (UKF). We discuss the observer model first.

a) Observer model: An approximate discrete-time continuous-state model is considered available as a description of the system of interest. We index the discrete time instants (t_k) with k ($k = 0, \ldots$) and assume a constant interval between them ($\Delta = t_{k+1} - t_k$). The observer model consists of two key components:

1) A discrete-time dynamic process model, accounting for a V-dimensional vector of unknown input disturbances ($\boldsymbol{v}_k$) and dynamics of the M-dimensional state vector ($\boldsymbol{x}_k$). We assume the following linear time-invariant state-space model for this purpose:

$$\begin{aligned} \boldsymbol{x}\left(t+\Delta\right) &= \boldsymbol{A}\,\boldsymbol{x}(t) + \boldsymbol{B}\,\boldsymbol{v}(t), \qquad \boldsymbol{x}\left(0\right) = \boldsymbol{x}_0, \\ v_i(t) &\sim \mathcal{N}\left(0,1\right), \qquad\qquad i = 1,\ldots,V \end{aligned} \tag{1}$$

2) A description of the offset ($b_j(t)$) for each of N sensors ($j = 1,\ldots,N$) as a stochastic process inspired by [6] that is equivalent to a Wiener process or Brownian motion:

$$\begin{aligned} b_j\left(t+\Delta\right) &= b_j(t) + w_j(t), \qquad b_j\left(0\right) = 0, \\ w_j(t) &\sim \mathcal{N}\left(0,\gamma_j\right), \qquad j = 1,\ldots,N \end{aligned} \tag{2}$$

where $w_j\left(t_k\right)$ is the input noise to describe the drift in sensor j and γ_j the associated standard deviation.

b) Measurement equation: We assume the available measurements ($\tilde{y}_j(t)$, $j = 1\ldots,N$) are chosen or designed to depend nonlinearly on the process state vector ($\boldsymbol{x}(t)$). They are also subject to a time-varying offset ($b_j(t)$) and additive measurement noise ($e_j(t)$):

$$\begin{aligned} y_j(t) &= a_j\, f_j\left(\boldsymbol{x}(t)\right), \\ e_j(t) &\sim \mathcal{N}\left(0,\sigma_j\right), \\ \tilde{y}_j(t) &= y_j(t) + b_j(t) + e_j(t) \qquad j = 1,\ldots,N \end{aligned} \tag{3}$$

The sensor gains (a_j) and the nonlinear response curves ($f_j\left(\cdot\right)$) are considered time-invariant in this study. In future work, we expect to allow the sensor gains to drift as well. We expect that the nonlinear response curve should remain time-invariant however for the method to work well.

c) Note on prior knowledge: The observer model is considered only an approximate model for the system of interest. The estimates of the parameters $\boldsymbol{A}$, $\boldsymbol{B}$, γ_j, and σ_j are not necessarily precise. They should however offer a sensible description of the dynamics of the monitored process and the sensor offsets. In contrast, the functions (f_j) describing the sensor responses are assumed known perfectly.

2) Observer:

a) Unscented Kalman Filter (UKF): To simultaneously estimate the process states ($\boldsymbol{x}(t)$) and the sensor offsets (b_j), we deploy the UKF. Our choice for the UKF in favor of the extended Kalman filter (EKF) is motivated by the fact that UKF can easily handle discontinuities in the sensor response curves. Indeed, the simulated sensor response curve in our simulation exhibit a discontinuous first derivative, which would challenge the use of the EKF.

We make use of the UKF described in Table 7.2 in [7] and describe only the essential elements here. The UKF, like any Kalman filter, tracks the evolution of the system states. In the present case, the system states are described with the augmented $M+N$-dimensional vector $\bar{\boldsymbol{x}}$ composed of the process state vector and the vector of sensor offsets:

$$\bar{\boldsymbol{x}} := \begin{bmatrix} \boldsymbol{x} \\ \boldsymbol{b} \end{bmatrix} \tag{4}$$

The UKF then proceeds by updating an estimate of the mean ($\hat{\bar{\boldsymbol{x}}}(t)$) and covariance matrix ($\Sigma_{\bar{x}}$) describing the above state vector each time a new an M-dimensional measurement vector ($\tilde{\boldsymbol{y}}$) is available:

$$\hat{\bar{\boldsymbol{x}}}\left(t_k\right), \Sigma_{\bar{x}}\left(t_k\right) \leftarrow \mathbf{UKF}\left(\hat{\bar{\boldsymbol{x}}}\left(t_{k-1}\right), \Sigma_{\bar{x}}\left(t_{k-1}\right), \tilde{\boldsymbol{y}}\left(t_k\right)\right) \tag{5}$$

$$\hat{\bar{\boldsymbol{x}}}\left(0\right) = \hat{\bar{\boldsymbol{x}}}_0 \tag{6}$$

$$\Sigma_{\bar{x}}\left(0\right) = \Sigma_{\bar{x},0} \tag{7}$$

where $\mathbf{UKF}\left(\cdot\right)$ represents the joint effect of the time and measurement updates on state estimate and covariance matrix from one time instant to the next. Within each update, the UKF simulates the process for a number of state vectors, named sigma points. These sigma points are sampled in a deterministic fashion. This sampling procedure is specified completely with a number of hyper-parameters, which are α, β, and κ. In our study, we set their values equal to $\alpha = 1$, $\beta = 0$, and $\kappa = 0$ and refer to [8] for more details.

3) Note on observability: A quick inspection of the observer shows that the number of states being estimated equals $M+N$ while only N measurements are available at each sampling time. For linear systems, the UKF will reduce to the Kalman filter and lead to a lack of structural observability [9]. At best, the system will be considered detectable. The main idea behind our approach is that the UKF can offer structural observability of all $M+N$ states if the sensor responses are nonlinear. A theoretical analysis specifying the exact conditions under which this is true is in progress. However, we illustrate below that practical observability of all states can be achieved if *(a)* the sensor response curves exhibit discontinuities of the first derivative and *(b)* if the system is sufficiently excited.

B. Simulation study

1) Simulated system:

a) Scenario A: To illustrate the proposed method, we simulate a simple hydraulic reservoir described with its water level as the single process state (h), so that $M = 1$. The reservoir has a constant horizontal cross-sectional area ($A = 1m^3$) and is fed with an unknown and unmeasured flow rate $q_{in}(t)$.

The outgoing flow rate depends on the tank level through a square-root dependency. The dynamics of the tank level are described through the following ordinary differential equation:

$$\dot{h}(t) = \frac{1}{A}\left(q_{in}(t) - q_{out}(t)\right) = \frac{1}{A}\left(q_{in}(t) - \sqrt{h(t)}\right) \quad (8)$$

The reservoir is monitored with $J = 3$ sensors measuring pressure in equivalent water height. Each sensor exhibits a time-varying offset $b_j(t)$ described by an integrated Brownian motion:

$$\begin{aligned} \dot{b}_j(t) &= \rho(t), & b_j(0) &= 0, \\ \dot{\rho}_j(t) &= \sigma\, w_j(t), & \rho_j(0) &= 0, \\ w_j(t) &\sim \mathcal{N}(0, \eta_j) \end{aligned} \quad (9)$$

where $\rho(t)$ defines the drift rate at time t and η is the input noise parameter describing its stochastic drift. Together, these equations describe the sensor offset drift as an time-integrated Wiener process. It is also a special case of the continuous-time local linear trend model [10]. In the present study, we use $\eta_j = 0.2\ mm/d^2$ for all sensors. Note that we use a different symbol to describe the stochastic drift in the simulated system (η) and in the observer model (γ) to stress the presence of model-reality mismatch.

The pressure sensors are mounted at a known and constant height above the reservoir bottom, named λ_j. In our simulations, they take values $\lambda_1 = 0$m, $\lambda_2 = 2$m, and $\lambda_3 = 4$m. The equations relating the noisy pressure measurement to the water level and the sensor offsets thus are:

$$\begin{aligned} p_j(t) &= \max\left(h(t) - \lambda_j, 0\right), \\ e_j(t) &\sim \mathcal{N}(0, \sigma_j), \\ \tilde{p}_j(t) &= p_j(t) + b_j(t) + e_j(t), \qquad j = 1, \ldots, N \end{aligned} \quad (10)$$

The flow rate $q_{in}(t)$ is simulated by means of a linear combination of two sine waves, one of which has a randomly varying amplitude:

$$\begin{aligned} q_{in}(t) &= a(t)\left(q_{in,0}(t) + q_{in,1}(t) + q_{in,2}(t)\right), \\ q_{in,0}(t) &= 4, \\ q_{in,1}(t) &= \sin\left(\tau\,\frac{t}{\theta_1} - \tau\,\frac{1}{4}\right), \\ q_{in,2}(t) &= 2\,\sin\left(\tau\,\frac{t}{\theta_2}\right), \\ a(t+\Delta) &= \begin{cases} \mathcal{U}(0,1), & \text{if: } \frac{t}{\theta_2} = \lfloor \frac{t}{\theta_2} \rfloor \\ a(t), & \text{otherwise} \end{cases} \end{aligned} \quad (11)$$

with $\theta_1 = 360$, $\theta_2 = 1$, and $\tau = 2\,\pi$. This input signal, while unknown to the observer, was designed such that the tank level $h(t)$ repeatedly crosses the mounting height of 2 of the 3 sensors (λ_2 and λ_3) during the simulated period. We return to this aspect below.

The system was simulated for a period of 360 days. Measurements are obtained every 15 minutes ($\Delta = 1/96$d), leading to $N = 34657$ measurement samples.

b) Scenario B and C: To further illustrate the value of discontinuous sensor response curve, we modify the sensor positions such that all sensors are at the bottom of the simulated tank, i.e. $\lambda_1 = \lambda_2 = \lambda_3 = 0$ m. By doing so, the water level in the tank can never cross any of the sensors' locations, which means all sensors respond in a perfectly linear way to the variable of interest. As will be shown below, this makes the drift of sensor offsets unobservable.

2) Observer model:

a) Scenario A and B: The model used for state estimation is an imperfect representation of true system that is simulated. We use the general representation of the observer model (1)-(3) and make it specific to the studied case by means of the following choices:

$$\begin{aligned} M &= 1, & N &= 3, \\ \boldsymbol{A} &= 1, & \boldsymbol{B} &= 100\,mm, \\ \gamma_j &= 1\,mm, & \sigma_j &= 1\,mm \qquad (j = 1, \ldots, J) \end{aligned} \quad (12)$$

b) Scenario C: A final modification of the setup is constructed by ignoring the sensor drift completely. Practically, this means the observer model is simplified by removing (2) and retaining (1) and (3) only. The offset terms ($b_j(t)$) are removed from (3). As in scenario B, the three sensors are placed at the bottom of the tank ($\lambda_1 = \lambda_2 = \lambda_3 = 0$ m). Consequently, the observer model is now completely linear so that the UKF, with values for the tuning parameters (α, β, κ) chosen above, reduces to the classical Kalman filter. The parameters that remain in the observer model (i.e., $\boldsymbol{A}$, $\boldsymbol{B}$) take the same values as before.

III. Results

A. System simulation

1) Scenario A: Figure 1 shows the simulated values for flow rate (panel (a)), the water level (panel (b)), the sensor offsets (panel (c)), and the noisy sensor measurements (panel (d)) in Scenario A. One can see in panel (b) that the experiment is designed so that the water level crosses the mounting positions of sensor 2 and 3 a number of times throughout the simulated period. Based on panel (c), one can also note that the worst sensor offset is recorded for sensor 3. This maximum offset is close to 1m in magnitude, roughly amounting to 10% of the maximum value attained by the water level. If one tracks the offset in the best-performing sensor, i.e. select the minimal magnitude of the three offsets at every sampling time, then one sees that the offset in the best-performing sensor is maximal on day 222 and produced by sensor 2.

2) Scenario B (not shown): The simulation results for scenario B look very similar to those of scenario A. The only exception is that the sensor signals never saturate in this. The simulated tank level and the sensor offsets due to accumulated drift are exactly the same however.

B. Observed-based drift fault correction

1) Scenario A: Figure 2 shows the results obtained through joint state estimation of the water level and the three sensor

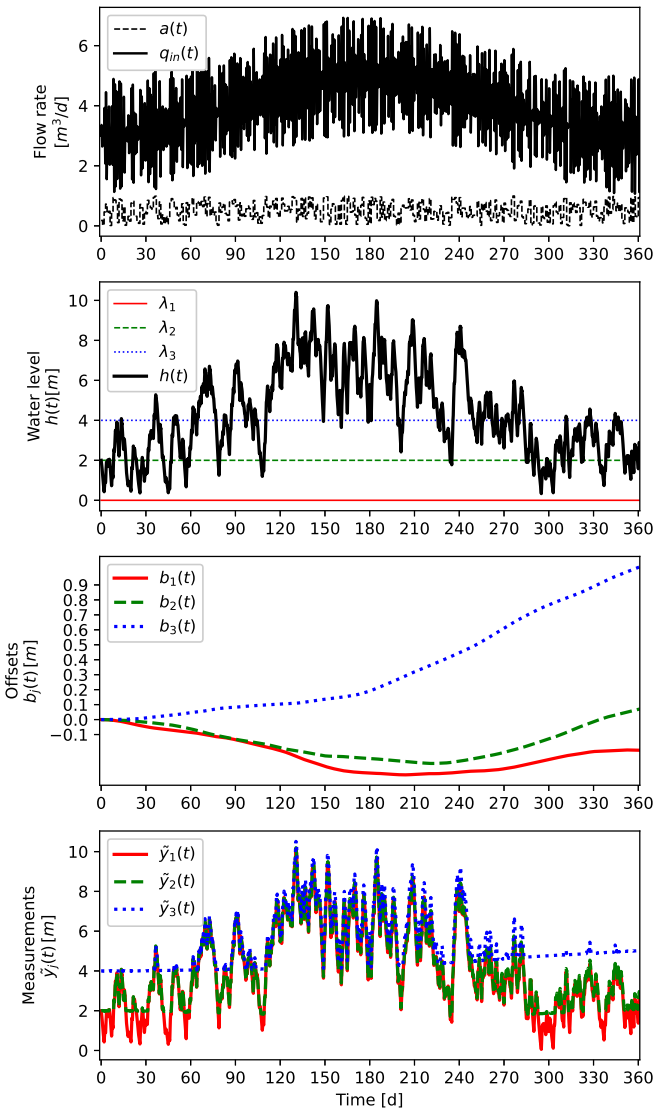

Fig. 1. System simulation – Scenario A. *(a)* Feed flow rate; *(b)* Water level *(c)* Sensor offsets; *(d)* Measurements.

offsets based on the UKF in scenario A. In panel (a), one can see that the estimated water level follows the trends in the true water level closely. Panel (b) offers more detail as it shows the estimation error as well as uncertainty bounds offered by the UKF. Here, one sees that the observer cannot track the true tank level perfectly. However, the estimation error remains below 0.07 m at all times, less than 10% of the worst offset and less than 1% of the maximum attained value. One can also see that the estimation error improves every time the true water level crosses the mounting height of sensor 2 or 3. Panels (c-e) show the true sensor offset as well as their estimates. As with the water level, the UKF is able to track the offsets fairly well, with estimation errors below 0.08 m at all times. The offset estimates generally improve when the water level crosses one of the sensor mounting positions.

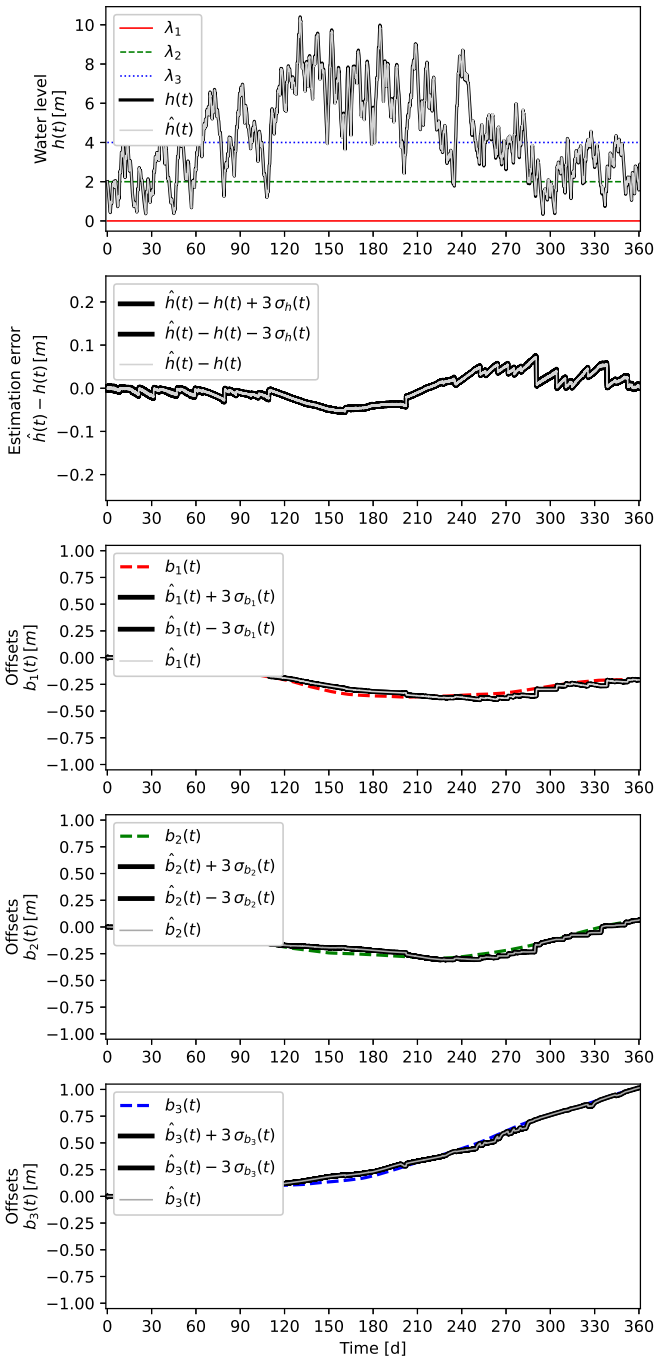

Fig. 2. Scenario A: State estimation with the UKF with sensors placed at distinct heights. *(a)* Water level - true and estimated values; *(b)* Water level estimation error with 3-σ uncertainty bands; *(c)* Sensor offset for sensor 1 - true and estimated values with 3σ bands; *(d)* Sensor offset for sensor 2 - true and estimated values with 3σ bands; *(e)* Sensor offset for sensor 3 - true and estimated values with 3σ bands.

2) Scenario B: Figure 3 shows the results obtained through joint state estimation of the water level and the three sensor offsets based on the UKF. In panel (a), one can see that the estimated water level follows the trends in the true water level. However, panel (b) shows that the estimation error can be as high as 0.25 m in magnitude. Thus, one sees that the observer cannot track the true tank level perfectly. Panels (c-e) show the true sensor offset as well as their estimates. As with the water level, the observer is unable to track variations in the offsets of the individual sensors. Instead, they appear to drift slowly without even tracking the trends on the true offset values. This clearly illustrates the value of the deliberate introduction of a discontinuous sensor response, specifically by placing the differential pressure sensors at heights within the range of level measurement.

3) Scenario C: Figure 4 shows the results obtained through state estimation of the water level based on the Kalman filter, thus ignoring drift of the sensor measurements. In panel (a), one can see that the estimated water level generally follows the trends in the true water level. However, panel (b) shows that the estimation error can be as high as 0.3 m in magnitude. As expected, the observer cannot track the true tank level perfectly. This further illustrates the need for the proposed method as a way to correct for sensor drift without human intervention.

IV. Discussion

With this contribution, we offer a first-time attempt at a systematic approach to detection and correction of incipient faults that appear simultaneously in a set of redundant sensors. We show that this is feasible through exploitation of a nonlinear response of the deployed sensors to the variable of interest. Such an automated method is especially valuable when human sensor validation and calibration cannot be afforded [11], [12] and could reduce the cost of sensor ownership significantly, even when regular maintenance efforts are supported.

As of now, the method requires the sensor response curves *(a)* to be known apart from an offset, *(b)* to be time-invariant, and *(c)* to exhibit at least one discontinuity in their first derivatives. We expect to relax some of these requirements in future work. Importantly, we do not need a precise model describing the system dynamics. For example, a linear discrete-time model was used to represent the true nonlinear continuous-time dynamic process in our simulation study. The method does require sufficient excitation of the variable of interest however, so that at least one of the discontinuities is detected regularly. Future theoretical analysis will be used to determine the precise conditions that need to be met to ensure reliable tracking of the sensor drift.

Our study leads to a curious shift in sensor design specifications. Conventionally, an ideal sensor is considered to respond linearly to the variable of interest in the expected range of measurement. For this reason, sensors are often designed and manufactured to exhibit a response that is as linear as possible. This desire is also apparent in sensor quality standards [13]. In contrast, our results suggest that selecting or designing sensors

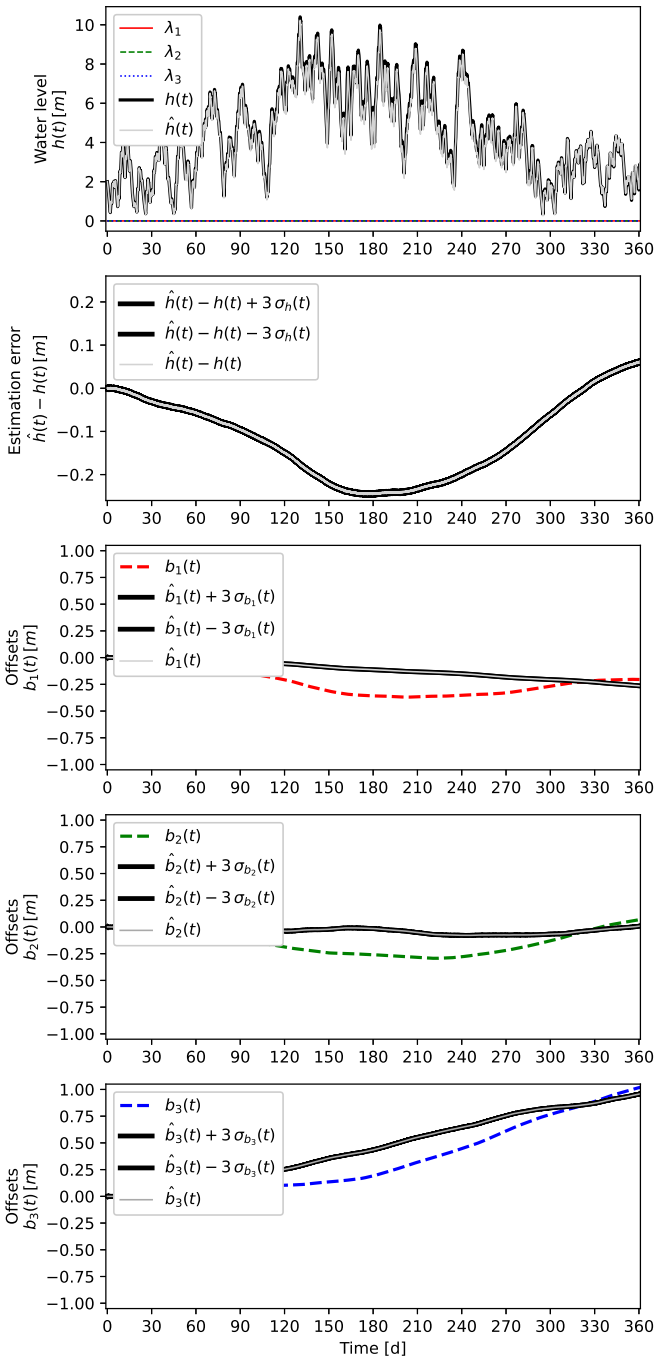

Fig. 3. Scenario B: State estimation with the UKF with sensors placed at the bottom of the tank. *(a)* Water level - true and estimated values; *(b)* Water level estimation error with 3-σ uncertainty bands; *(c)* Sensor offset for sensor 1 - true and estimated values with 3σ bands; *(d)* Sensor offset for sensor 2 - true and estimated values with 3σ bands; *(e)* Sensor offset for sensor 3 - true and estimated values with 3σ bands.

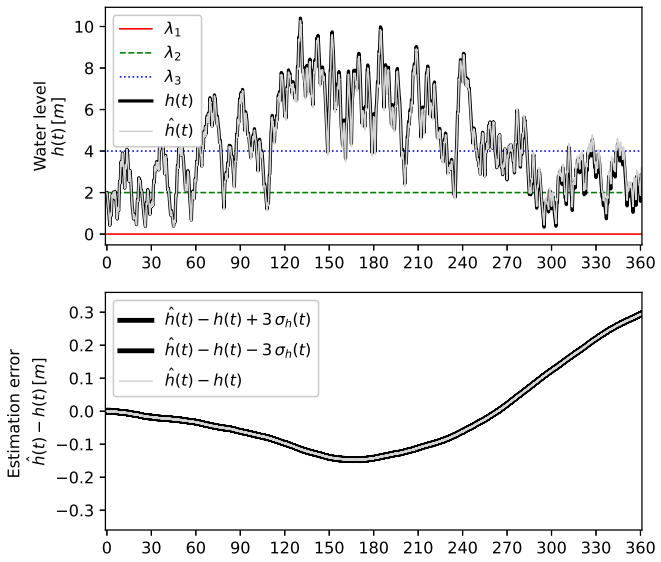

Fig. 4. Scenario C: State estimation with the Kalman filter with sensors placed at the bottom of the tank. *(a)* Water level - true and estimated values; *(b)* Water level estimation error with 3-σ uncertainty bands.

so that they exhibit a discontinuous or otherwise nonlinear response curve can be desirable. To our knowledge, this is the only known way to automatically detect and correct for drift in sensors that drift simultaneously and similarly.

The proposed method depends critically on the excitation of the variable of interest. In the present study, this was achieved through a dynamic simulation of the unmeasured and uncontrolled input disturbances. In practice, the disturbances may of insufficient to generate the necessary excitation. Future work will therefore focus on ensuring sufficient excitation, e.g., through use of online optimal experimental design methods or dual control [14].

Finally, the UKF is not the only approach amenable to simultaneous estimation of all sensor offsets. We predict that other methods, like moving horizon estimation (MHE), are useful as well. This will be explored in future work.

V. Conclusions

These are our main conclusions:

1) A novel method for automatic correction of offset drift occurring simultaneously in multiple sensors measuring the same state variable is proposed. The method is based on the unscented Kalman filter for joint estimation of the variable of interest and the sensor offsets and exploits nonlinear behavior of the deployed sensors to this end.
2) The method fits nicely into the toolbox for resilient monitoring and control. The proposed approach is considered a self-healing approach for sensor network management.
3) Our work highlights a possible shift in sensor design thinking. Rather than focusing on the design and maintenance of a linear sensor response, there is clear value in designing sensors that exhibit nonlinear yet time-invariant features within the measurement range.

References

[1] F. Blumensaat, J. P. Leitão, C. Ort, J. Rieckermann, A. Scheidegger, P. A. Vanrolleghem, and K. Villez. How urban storm-and wastewater management prepares for emerging opportunities and threats: digital transformation, ubiquitous sensing, new data sources, and beyond - a horizon scan. *Environmental Science and Technology*, 53(15):8488–8498, 2019.

[2] S. Sagiroglu and D. Sinanc. Big data: A review. In *IEEE 2013 international conference on collaboration technologies and systems (CTS)*, pages 42–47, 2013.

[3] O. Y. Al-Jarrah, P. D. Yoo, S. Muhaidat, G. K. Karagiannidis, and K. Taha. Efficient machine learning for big data: A review. *Big Data Research*, 2(3):87–93, 2015.

[4] F. Harrou, Y. Sun, A. S. Hering, M. Madakyaru, and A. Dairi. *Fault Isolation*, chapter 3, pages 71–117. Elsevier, 2021.

[5] K. Ohmura, C. M. Thuerlimann, M. Kipf, J. P. Carbajal, and K. Villez. pH sensor ageing experiment (SoDAN-dataset1), 2019.

[6] Kito Ohmura, Christian M. Thürlimann, Marco Kipf, Juan Pablo Carbajal, and Kris Villez. Characterizing long-term wear of ion-selective ph sensors. *Water Science and Technology*, 80(3):541–550, 2019.

[7] S. Haykin. *Kalman filtering and neural networks*. John Wiley & Sons, New York, NY, USA, 2001.

[8] E. A. Wan and R. Van der Merwe. The unscented Kalman filter for nonlinear estimation. In *Proc. Symp. Adaptive Syst. Signal Process, Commun. Contr., Lake Louise, AB, Canada, Oct. 2000.*, 2000.

[9] Z. Gajic and M. Lelic. *Modern control systems engineering*. Prentice-Hall, Inc.., 1996.

[10] A. C. Harvey. *Forecasting, Structural Time Series Models and the Kalman Filter*. Cambridge University Press, Cambridge, UK, 1989.

[11] M. Y. Schneider, J. P. Carbajal, V. Furrer, B. Sterkele, M. Maurer, and K. Villez. Beyond signal quality: the value of unmaintained ph, dissolved oxygen, and oxidation-reduction potential sensors for remote performance monitoring of on-site sequencing batch reactors. *Water Research*, 161:639–651, 2019.

[12] M. Y. Schneider, V. Furrer, E. Sprenger, J. P. Carbajal, K. Villez, and M. Maurer. Benchmarking soft sensors for remote monitoring of on-site wastewater treatment plants. *Environmental Science abd Technology*, 54(17):10840–10849, 2020.

[13] ISO. *ISO15839: On-linesensors/analysing equipment for water - Specifications and performance tests*. International Standards Organization, 2003.

[14] A. Mesbah. Stochastic model predictive control with active uncertainty learning: A survey on dual control. *Annual Reviews in Control,*, 45:107–117, 2018.